IEEE Access
Multidisciplinary | Rapid Review | Open Access Journal

Received March 31, 2020, accepted April 22, 2020, date of publication May 8, 2020, date of current version July 3, 2020.

Digital Object Identifier 10.1109/ACCESS.2020.2993235

Design Approaches and Control Strategies for Energy-Efficient Electric Machines for Electric Vehicles–A Review

LINGYUN SHAO[1], AHU ECE HARTAVI KARCI[1], DAVIDE TAVERNINI[1], ALDO SORNIOTTI[1], (Member, IEEE), AND MING CHENG[2], (Fellow, IEEE)

[1]Centre for Automotive Engineering, University of Surrey, Guildford GU2 7XH, U.K.
[2]School of Electrical Engineering, Southeast University, Nanjing 210096, China

Corresponding author: Aldo Sorniotti (a.sorniotti@surrey.ac.uk)

This work was supported by the European Union's Horizon 2020 Program through the TELL Project under Grant 824254.

ABSTRACT The market penetration of electric vehicles (EVs) is going to significantly increase in the next years and decades. However, EVs still present significant practical limitations in terms of mileage. Hence, the automotive industry is making important research efforts towards the progressive increase of battery energy density, reduction of battery charging time, and enhancement of electric powertrain efficiency. The electric machine is the main power loss contributor of an electric powertrain. This literature survey reviews the design and control methods to improve the energy efficiency of electric machines for EVs. The motor design requirements and specifications are described in terms of power density, efficiency along driving cycles, and cost, according to the targets set by the roadmaps of the main governmental agencies. The review discusses the stator and rotor design parameters, winding configurations, novel materials, construction technologies as well as control methods that are most influential on the power loss characteristics of typical traction machines. Moreover, the paper covers: i) driving cycle based design methods of traction motors, for energy consumption reduction in real operating conditions; and ii) novel machine topologies providing potential efficiency benefits.

INDEX TERMS Electric machine, electric vehicle, efficiency, power loss, design parameters, control methods, driving cycle.

I. INTRODUCTION

Socio-economic factors and technological advances are making electric vehicles (EVs) more and more competitive for mainstream transportation. To maintain this EV momentum, great effort is ongoing to further develop energy-efficient electric propulsion systems and their primary components [1], [2], i.e., batteries, power electronic devices, and electric machines (EMs), and to make them commercially viable for production EVs.

In general, the operating voltage of electrified powertrains has been increasing in recent years, because of the associated reduction of the current levels and power losses [2], [3], and the cost benefits in terms of connectors, cables and power semiconductors [4]. In specific applications, e.g., in the Toyota hybrid system [5], bi-directional converters have been used to boost the battery voltage. This kind of high voltage DC/DC converters can increase efficiency by adjusting the DC-bus voltage [6]. However, new challenges regarding insulation requirements, reliability, safety and efficiency of components arise as extremely high voltage systems are used in new EVs [6]–[8].

Table 1 illustrates the main specifications of several representative EV models. With the largest passenger car market, China stood for 53% of the global sales of EVs and plug-in hybrid electric vehicles in 2019 [9], e.g., see the Chinese top selling EV models by BYD, BAIC BJEV, SAIC Motor, Geely, Chery, and JAC. The majority of production EVs have a centralized on-board powertrain layout with one EM per axle, which is connected to the two wheels through a mechanical transmission with differential, half-shafts, and constant velocity joints. For premium segment EVs, all-wheel-drive (AWD) configurations with two EMs (one per axle) are the latest trend,

The associate editor coordinating the review of this manuscript and approving it for publication was Christopher H. T. Lee.

TABLE 1. Representative production EVs and their main EM characteristics.

EV models	Motor type	Max power (kW)	Max torque (Nm)	Top speed (km/h)	Drive type	Year
Tata Nexon EV[24]	PM	85	200	-	FWD	2020
Porsche Taycan Cross Turismo[25]	-	440*	900*	250	AWD	2020
Honda e advance[25]	-	113	315	145	RWD	2020
Volkswagen id.3[25]	PM	100	275	160	RWD	2020
Kia e-Soul[25]	PM	100	395	156	FWD	2020
Volkswagen e-golf[25]	PM	100	290	150	FWD	2019
BYD S2[27]	PM	70	180	101	FWD	2019
BJEV EX3[28]	PM	160	300	150	FWD	2019
JAC iEVS4[29]	PM	110	330	150	FWD	2019
Smart EQ fortwo[30]	PM	60	160	130	RWD	2019
Mercedes EQC[31]	IM+IM	300*	760*	180	AWD	2019
Kia e-Niro[32]	PM	150	395	167	FWD	2019
Roewe Marvel X[27]	3 PMs	222*	665*	170	AWD	2018
Hyundai Kona Electric[33]	PM	150	395	167	FWD	2018
Audi e-tron[10]	IM+IM	125+140	247+314	200	AWD	2018
Jaguar I-PACE[11]	PM+PM	147+147	348+348	200	AWD	2018
Tesla Model 3[12]	IM+PM	147+211	639*	260	AWD	2018
Renault ZOE[37]	SynC	80	225	135	FWD	2018
JAC iEV7L[29]	PM	50	215	110	FWD	2017
BJEV EC180[34]	IM	30	140	100	FWD	2016
Geely Emgrand EV[26]	PM	120	250	140	FWD	2016
Tesla Model S P85D[35]	IM+IM	165+350	931*	250	AWD	2016
BMW i3[36]	PM	125	250	150	RWD	2016
Chery eQ[27]	PM	41.8	150	100	FWD	2015
Fiat 500e[38]	PM	83	200	141	FWD	2013
Roewe E50[27]	PM	52	155	130	FWD	2013
Mercedes SLS[39]	4 PMs	552*	1000*	250	AWD	2013
Nissan Leaf[21]	PM	80	280	145	FWD	2012
BYD e6 EV[27]	PM	90	450	140	FWD	2008
Tesla Roadster[40]	IM	185	200	200	RWD	2008

Notes. AWD: all-wheel-drive; RWD: rear-wheel-drive; FWD: front-wheel-drive; SynC: synchronous machine with rotor coils; *: combined value.

because of their intrinsically better traction and handling performance [10]–[12]. In these configurations, the two machines can target different objectives, e.g., one machine can be optimized for energy efficiency during normal use, while the second one provides the required traction torque/power performance. For example, this is the choice of Tesla for the Model 3, which combines an induction machine (IM) and a permanent magnet (PM) machine [13].

As core components of electric propulsion systems, EM technologies have been extensively researched in terms of motor topologies, basic characteristics, control strategies and operating performance evaluations [14]–[18]. In the last 20 years, IMs have been the most popular EM type for EVs, because of their low cost, high reliability, and mature manufacturing and control techniques [14], [15]. However, PM synchronous machines tend to have higher torque density and efficiency than IMs, and thus are becoming increasingly attractive for EVs [14], [16]. In particular, interior PM (IPM) motors for passenger car applications have higher overload capability and efficiency than IMs and surface-mounted PM (SPM) machines [15], [17]. This justifies the adoption of IPM machines in many EVs or hybrid electric vehicles (HEVs) on the market, including the Honda Accord [19], Toyota Prius [20], and Nissan Leaf [21]. The key problem of PM machines is the rapid and significant fluctuation of the price of rare-earth materials. Therefore, intensive research is ongoing on synchronous machines with reduced or absent rare-earth materials [22], which has led to the development of the PM-assisted synchronous reluctance (PMaSynR) machines.

To increase EV mileage, energy efficiency is key in electric powertrains. EM efficiency is influenced by many factors, which include the machine type, topology and geometry, control strategy, material and manufacture technology, as well as cooling conditions. Different methods have been proposed to improve the efficiency of EV motors. For instance, soft magnetic lamination materials, nano-material based conductors and high energy product PMs are discussed in [23], to reduce iron and copper losses. However, to the authors' best knowledge, there are no published articles that comprehensively summarize the design and control methods to improve the energy efficiency of EV machines.

To cover the gap, after discussing the typical EM specifications for EVs in Section II, this survey provides guidelines to improve the energy efficiency of typical traction machines for electric passenger cars, and focuses on: i) the main geometries, materials and construction techniques that have direct or indirect effect on efficiency (Section III); ii) control strategies for EM power loss minimization at each given torque and speed (Section IV); and iii) driving cycle based EM design methods for minimizing the energy loss along the actual mission profile (Section V). Moreover, Section VI presents recent advances in EV motor topologies and designs, which have potential to improve electric powertrain efficiency, whilst Section VII draws the main conclusions.

The cited academic papers give a comprehensive explanation and analysis of the main reviewed aspects, whilst the web based references, including product brochures and technical reports, provide solid data to show the current state-of-the-art of EV motors.

II. ELECTRIC MACHINE SPECIFICATIONS FOR ELECTRIC VEHICLES

Several governmental agencies have analyzed the current and expected future trends in terms of traction motor performance. For example, the 2018 electric machine roadmap

TABLE 2. Performance targets for EV traction machines according to the UK APC and US DoE roadmaps.

Passenger car EM targets	UK APC			US DoE	
	2017	2025	2035	2020	2025
Inverter voltage (V) / current (A)	**350/450**			**325/400**	**650/600**
Cost ($/kW)	10	5.8	4.5	4.7	3.3
Continuous specific power (kW/kg)	2.5	7	9	1.6	5
Continuous power density (kW/l)	7	25	30	5.7	50
Efficiency (%)	86.5[1]	92.5[1]	93[1]	>95[2]	>97[2]

Notes. [1]: Average EM efficiency along the WLTP [44]; [2]: Maximum EM efficiency.

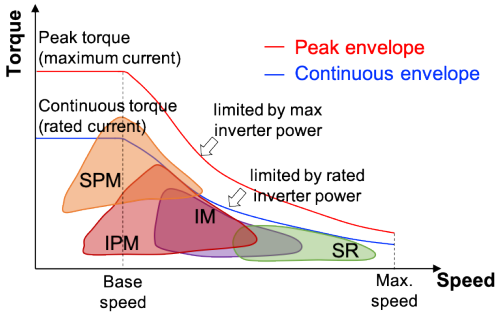

FIGURE 1. Motor torque-speed characteristics and qualitative overlay of premium efficiency regions for IMs, SR motors, SPM motors and IPM motors for EVs (extrapolation of results from [2], [15], [17], [18], [62]).

of the UK Advanced Propulsion Centre (APC) [41] sets the targets in Table 2 for passenger car traction motors, with respect to their cost, specific power, power density and efficiency. Also the US Department of Energy (DoE) sets targets for EV traction machines, to be achieved by 2020 and 2025 [42]. The DoE document states that their previous electric powertrain targets were based on 55 kW peak and 30 kW continuous power levels, under the assumption of a 325 V battery voltage and a 400 Arms maximum inverter current. As car makers are moving forward with larger and heavier EVs, in the 2017 release of the US DoE roadmap, the 2025 baseline peak and continuous power values were respectively increased to 100 kW and 55 kW, with 650 V battery voltage and 600 Arms inverter current. From 2020 to 2025, the DoE guidelines target 30% cost reduction, 89% volume reduction, and maximum efficiency increase from >95% to >97%. Moreover, at any speed the torque ripple should be <5% of the peak torque [42], [43]. The electrification roadmap of the European Road Transport Research Advisory Council (ERTRAC) sets motor-to-wheel efficiency target ranges for 2030, i.e., 86-91% along the new European driving cycle (NEDC), and 87-92% along the worldwide harmonized light vehicles test procedure (WLTP) [44], [45], which represent only a 1% increase from the respective values for 2016. With the rapid development of the national EV industry, the Chinese government also sets indicators for next generation EV machines, e.g., peak power density >4 kW/kg and peak efficiency >96%, to be achieved by 2020 [46].

In general, desirable characteristics for EV traction motors are: i) high torque capability at low speed for acceleration and hill climb performance; ii) constant-power speed range of 3-4 times the base speed, as a compromise between peak torque requirement and inverter power rating; iii) high efficiency over a wide operating range; iv) intermittent overload capability; v) high specific power for EV mass reduction and range extension; vi) high power density for ease of powertrain packaging; and vii) low cost [14]. As the EM torque ripple participates in generating noise, vibration and harshness, restricting its magnitude is also important. During the design phase, the trade-off relations between the previous characteristics should be investigated and quantified through appropriate models. Table 3 presents EM test results from benchmarking evaluations of typical commercial electric powertrains, carried out for the 2005 Honda Accord [19], 2010 Toyota Prius [20], 2012 Nissan Leaf [21], and 2016 BMW i3 [22] by the Oak Ridge National Laboratory (ORNL), as well as available data for multiple traction machines [47]–[57], among which the Bosch SMG 180/120 has been used in the Fiat 500e and Smart EQ fortwo.

The electric powertrain torque limits are generally represented as functions of speed, see Figure 1, and depend on the EM design, inverter current capability, and cooling arrangement. The EM must be capable of uninterruptedly operating under the continuous envelope without reaching its thermal limits. Therefore, temperature assessments on the hotspots at the base speed and maximum speed of the continuous envelope are crucial during motor design [43]. Besides, a mechanical analysis should be performed to ensure structural integrity of the rotor at the top speed. The powertrain peak torque, generally designed for transient overload operation, i.e., for matching the expected EV acceleration and hill climb performance, is typically twice the rated torque, according to [14]. The duration of the peak torque operation is limited by the temperatures of the motor windings, PMs and inverter, which are monitored by sensors, see the test reports of the 2010 Prius [20] and BWM i3 [22]. The first generation of the Nissan Leaf adopted a combination of measurement and estimation of the inverter temperatures to decide the powertrain torque limit [21].

The thermal management system is essential for motor performance, since machine efficiency and life expectancy are governed by the magnetic losses and heat generation [58]. As stated in [59], an appropriate cooling system boosts the EM performance, and allows motor size reduction, which in turn lowers vehicle weight and increases energy efficiency. In [60] better cooling, which reduces the coil temperature, leads to 0.25% and 0.50% increases in IM efficiency at 100% and 125% of the nominal load. The level of sophistication of the cooling system depends on the power density of the machine, which is expected to significantly increase in the next few years, according to the roadmaps in Table 2. Different cooling set-ups and design calculation methods applicable to automotive traction motors are reviewed in [58]. The cooling system should be designed according to the installation

TABLE 3. Examples of published data of EV traction motors.

Item	Unit	Accord 2005	Prius 2010	Leaf 2012	BMW i3 2016	Punch Powertrain EP2	McLaren E-motor	Siemens SIVETEC MRI	Siemens SIVETEC MRS	Bosch SMG 180/120	JJE OD220	JEE 90kW	Yasa P400 RS	Zytek 55kW	TM4 Motive MV275	Protean Pd18	Elaphe L1500D
Reference	-	[19]	[20]	[21]	[22]	[47]	[48]	[49]	[49]	[50]	[51]	[52]	[53]	[54]	[55]	[56]	[57]
Motor type	-	IPM	IPM	IPM	IPM	SR	SPM	IM	PM	PM	PM	PM	Axial Flux	PM	Outer SPM	Outer PM	Outer PM
PM shape	-	tangent	V	delta	tangent	-	-	-	-	-	-	-	-	-	-	-	-
Cooling	-	passive	liquid	liquid	liquid	-	liquid	liquid	liquid	liquid	liquid	liquid	liquid	liquid	liquid	liquid	liquid
Stator mass	kg	12.5	16.0	-	20.2	-	26[b]	-	-	32[b]	54[b]	-	28.2[b]	62[a]	42[b]	36[a]	34.8[b]
Rotor mass	kg	10.0	6.7	16.5	14.2	-		-	-			-					
Max torque	Nm	136	207	280	250	180	130	350	350	198	270	230	370	120	275	1250	1500
Max power	kW	12.4	60	80	125	>120	120	200	200	80	140	90	160	55	120	80	110
Top speed	rpm	6000	13500	10390	11400	20000	17000	20000	15000	12000	14000	12000	8000	12000	11000	1600	1516
Specific power	kW/kg	0.53	1.6	1.4	3.0	-	4.6*	-	2.6	2.5*	>4.2	-	6.7	-	2.86*	-	3.16*
Power density	kW/l	1.51	4.8	4.2	9.1	-	-	-	-	9.5*	-	-	-	-	-	-	-
Max efficiency	%	95	96	97	94	>92[a]	96	95	96.5	97	96	-	96	-	-	91[a]	94

Notes. *: Estimated data; [a]: Including motor and inverter; [b]: Assembled motor mass. Although the Honda Accord and Toyota Prius are HEVs, they have been included given the high availability of data for their EMs. The Protean Pd18 and Elaphe L1500D are in-wheel direct drive machines.

conditions of the motor, while considering cooling efficiency, reliability, manufacturing complexity, and maintenance cost.

The torque-speed map showing EM efficiency as a function of speed and torque is a useful tool for motor evaluation and design [61]. However, these maps are usually generated from steady-state efficiency measurements or simulations, which are incomplete for energy consumption evaluation in applications characterized by highly dynamic torque-speed variations. This issue is discussed in [62], where the dynamic efficiency is computed from the instantaneous input and output power levels at every sample point in a driving cycle. For high performance EVs, including many of those in Table 1, the powertrain yields high maximum torque values with respect to the typical driving cycle requirements, and therefore generally operates in its low torque region. For these applications, the efficiency at very low torque demand, although rarely measured, is essential to accurately predict EV consumption during realistic operation.

III. EM DESIGN PARAMETERS

The efficiency characteristics are predominantly determined by the machine type. Figure 1 overlays the typical high efficiency regions for four EV machine types [62], i.e., IMs, switched reluctance (SR) machines, as well as SPM and IPM machines. For IMs, the efficiency reaches its maximum at relatively high speed and low torque [2], and significantly decreases from its peak because of the important stator copper and rotor cage losses. According to [15], IMs are "penalized by the cage losses at both low and high speeds" compared to PM machines. According to [18], the SR machine is associated with lower efficiency values, and yields its maximum efficiency at higher speeds than its PM and IM counterparts designed under the same specifications. In comparison with IPM machines, SPM machines are easier to manufacture and have lower copper loss at low speeds, because of their short end turns [17]. However, the efficiency is penalized by the extra copper losses for PM flux weakening, and the PM losses at high speeds.

Although the shape of an EM efficiency map is predominantly determined by the machine type, subtle changes can be made through control modifications and parametric design compatible with the manufacturing constraints, to influence the resulting EM efficiency characteristics. Some of these parameters are common among different EM types, but many of them are motor topology specific. The selection of the most influential parameters is essential for fast and successful convergence to energy efficient design. The following sub-sections discuss leading design parameters, geometries, materials and manufacturing techniques for the four most relevant types of EV machines, i.e., IMs, PM synchronous machines, SR machines and PMaSynR machines.

A. INDUCTION MACHINES

IM technologies are mature and robust; however, the overload capability of IMs is restricted by the important heat dissipation in the rotor, which requires appropriate air cooling [15]. In IMs, the dominant losses are the copper losses in both stator and rotor, which decrease at high speeds because of the reduced magnetization current for flux weakening [18]. The iron loss initially increases with speed, and reaches its maximum at the base speed; then it gradually decreases in the flux weakening region. It is desirable to have similar iron and copper losses to maximize efficiency for each operating point [63]. Continuous efforts have allowed to achieve significant IM efficiency improvements through geometry design, materials, and construction techniques, in coordination with suitable slip control.

The design and requirements of the inverter-fed IMs used in EVs are different from those of traditional IMs without inverter. In fact, in conventional IMs, deep slots (Figure 2(a))

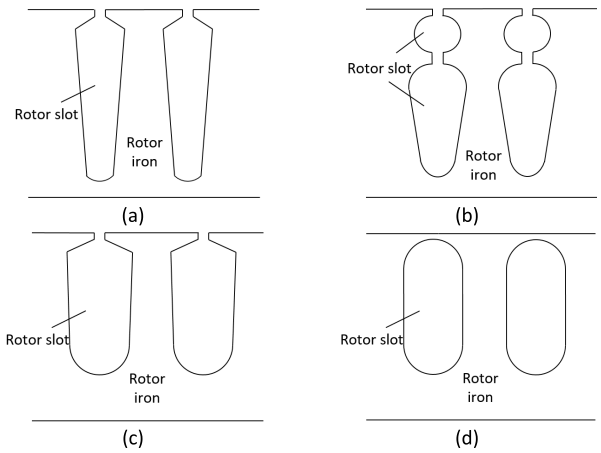

FIGURE 2. Typical rotor slot shapes of IMs: (a) Deep slots, (b) Double-cage slots, (c) Shallow and wide slots, (d) Closed slots (adapted from [64]).

or double-cage slots (Figure 2(b)) are employed to produce a variable rotor resistance, which is high at low speed to limit the starting current and boost the starting torque, but low at the rated speed for high efficiency. For inverter-fed IMs, the desired maximum starting torque can be easily achieved by adjusting voltage and frequency. Therefore, shallow and wide rotor slots (Figure 2(c)), which result in low rotor resistance and rotor leakage inductance, are suggested in [64] to keep high efficiency and power factor in a wide frequency range. However, the negative influence of high-order harmonics from the inverter should be considered in the design process. In this respect, reference [63] suggests closed or half-closed rotor slots to decrease the high-order air-gap harmonic magnetic fields, and thus to restrain the harmonic winding losses. Besides, it is favorable to have relatively high and similar numbers of stator and rotor slots, with the number of rotor slots lower than that of stator slots. In [65] closed rotor slots with round bottoms (Figure 2(d)) were used in an inverter-fed IM with a die-casting copper squirrel cage rotor for a small commercial EV, achieving a maximum efficiency of 94.4%, and a wide operating region with efficiency >93%.

Die-cast copper rotors are a proven technology to increase IM efficiency by 1%-2% with respect to the common aluminum rotors, by reducing the rotor ohmic losses because of the better conductivity [66]. This solution has been implemented in the Tesla EV motors, e.g., in the Model S. However, these rotors pose manufacturing challenges related to the tooling stresses and thermal shocks caused by the higher melting point [66].

B. PM SYNCHRONOUS MACHINES

PM synchronous machines have relatively recently become attractive to the traction motor market for EV/HEV applications. The PM brushless machine topologies can be categorized as SPM or IPM, respectively with magnets on the rotor surface and inside the rotor, see Figure 3. In PM machines, copper losses are dominant at low speeds, while iron losses

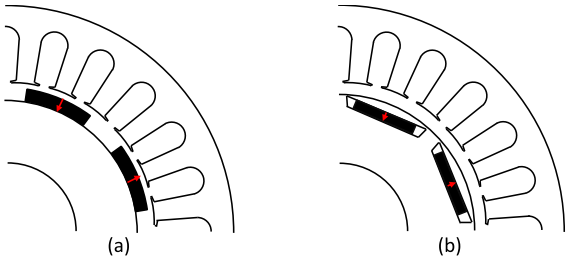

FIGURE 3. Alternative PM machine topologies with magnets on the rotor: (a) SPM, (b) IPM (adapted from [14]).

are prevalent at high speeds [61]. Furthermore, the harmonic iron loss induced by the PM harmonic fields becomes evident under flux weakening operation [67]. The rotor loss is relatively small compared with the stator copper and iron losses [14], however it is not negligible, especially in high frequency conditions, i.e., at high speed and/or with high pole number. The EM design process should prioritize the dominant loss component, according to the specific operating region of the machine.

The numbers of poles and slots have high impact on the EM performance and dimensions. Reference [68] gives analytical instructions for choosing suitable pole and slot combinations for fractional-slot SPM machines to achieve low rotor losses, i.e., it indicates 2.5 or 1.5 slots per pole for double-layer winding configurations, and 1.5 or 1 slots per pole for single-layer winding configurations. In both configurations, for a given slots per pole ratio, the rotor losses continue to decrease as the number of slots increases. In [69] a 14-pole SPM machine achieves 13.3% lower energy consumption along the new European driving cycle (NEDC) than its 10-pole counterpart. Moreover, a large inductance, achieved by increasing the number of turns and proportionally reducing the axial length of the motor, improves the flux weakening capability, and reduces the copper loss at high speeds. In [69] a design with 14% higher number of turns and 13% shorter axial length yields a 5% energy consumption reduction along the NEDC than the corresponding machine with the same flux linkage and torque production capability. However, the power factor and inverter rating may be compromised.

Great progress has been made with respect to the design and manufacture of the stator windings. The concentrated winding configuration has been employed in EMs for HEVs, such as the Honda Accord [19] and Chevrolet Volt [70], due to the benefits of high slot fill factor, short end-turn length and, thus, simple winding installation, better packaging and reduced copper loss [70]. However, this configuration brings high magnetomotive force (MMF) harmonics, which induce significant PM eddy-current losses and penalize efficiency at high speeds [71]. An effective mitigation measure is the circumferential or axial segmentation of the magnets [14]. Another design trend is based on bar-wound (or hairpin) flat-wire windings, which allow higher slot fill factor, shorter end windings, and better thermal behavior than the traditional stranded round-wire windings. Bar-wound windings have

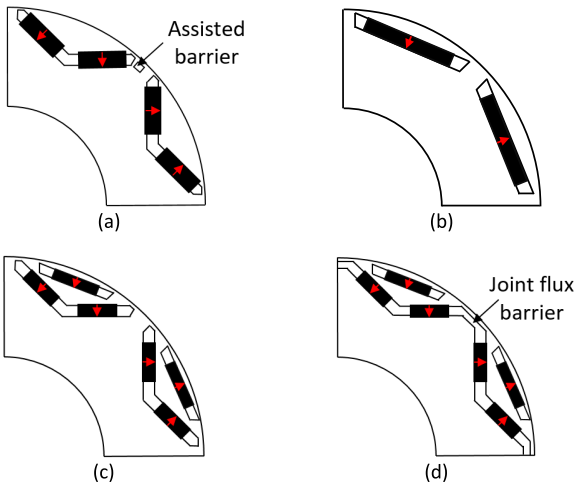

FIGURE 4. PM arrangements in IPM machine rotors: (a) V-shaped, (b) Tangential-type, (c) Delta-shaped, (d) Delta-shaped with joint flux barrier (adapted from [73], [78]).

been employed in production motors, such as those of the 2017 Toyota Prius, Chevrolet Volt, and Roewe Ei5. In particular, in the Chevrolet Volt, an efficiency improvement up to 5% in the low to medium speed range is achieved through the bar-wound construction [70]. However, this benefit can be compromised by the skin and proximity effects in the solid stator bars at high speeds. Therefore, specific connection schemes are proposed in [72] to limit the additional losses.

The PM arrangement in the rotor is essential for limiting losses in IPM machines. The tangential-type, V-shaped, and delta-shaped PM orientations (see Figure 4) have been employed in commercial EV motors, see Table 3. As discussed in [73], the V-shaped and tangential-type arrangements benefit from high efficiency and low torque ripple, respectively. However, the efficiency decreases with the increase of the width of the magnetic bridge between the two V-shaped magnets [73]. The EMs of the Nissan Leaf and 2017 Toyota Prius adopt delta-shaped PM arrangements to increase the reluctance torque and improve the high-speed flux weakening operation [74]. In comparison with the V-shaped topology, the delta-shaped design has higher torque capability and efficiency in the constant torque region, but lower efficiency in the flux weakening region [75]. A careful design is required on the width of the central bridge and the shape of the flux barriers at both ends of the magnets to restrict the effects of the harmonics and maintain the required mechanical strength [73], [75].

The design aspects of rotor flux barriers and their effects on machine performance, including torque capability, torque ripple and efficiency, are summarized in [76]. The authors of [77] added assisted barriers to one side between adjacent poles (see Figure 4(a)) in V-shaped-rotor IPM machines, to increase the contributions from the magnetic and reluctance torques. Compared to the proposed design, the efficiency is increased by 6.3%, because of the higher torque and lower iron losses. Joint flux barriers (Figure 4(d)) are adopted in delta-shaped IPM machines to block the harmonic flux through the path between the magnets, and reduce the PM eddy-current loss [78]. Trapezoidal magnets and rectangular magnets with triangular barriers are effective in reducing the harmonic iron loss in tangential-type IPM machines [67]. In [79] a non-uniform airgap geometry reduces the effect of the MMF harmonics on the iron losses, which are decreased by up to 50% at high speeds, with respect to a conventional machine with a uniform airgap.

C. SWITCHED RELUCTANCE MACHINES

SR machines are widely investigated for EVs because of their simple and robust structure, wide constant power capability and potentially low cost. With no PMs on the rotor, SR machines are suitable for high-speed operation because of the low centrifugal force on the rotor [80]. The main restrictions are their high torque ripple and acoustic noise, low power factor, and complex control [81]; however, the recent literature on SR machines shows notable advances in all these areas [82]–[84].

The most effective method to improve torque density and efficiency is to use iron materials with high saturation flux density and low iron loss, such as cobalt-iron-type materials, Super Core 6.5% silicon steel, and amorphous iron [85], [86]. In [85], an SR machine is designed to have a 96% maximum efficiency, which is comparable to the one of the 2009 Prius IPM machine, by employing 6.5% high silicon steel, a thinner iron sheet and a smaller airgap. Enhanced torque/power density and efficiency are expected with higher numbers of stator and rotor poles and smaller airgap length, at the price of reduced constant power and overload capabilities [81]. Besides, as pointed out in [86], the 24-16 stator-rotor pole geometry produces much lower acoustic noise than the 6-4 or 8-6 configurations. Moreover, narrower and longer poles bring wider constant power range and increase high speed efficiency, while slightly sacrificing rated torque and power [81]. However, these designs imply tight manufacturing tolerances.

The operation of SR machines relies on precise control, which should be compliant with the winding configuration. Reference [84] shows that for sinusoidal current excitation, the double layer short pitched winding has the highest efficiency, whereas for single layer short pitched winding, the unipolar excitation current with 180° electrical conduction period provides the highest efficiency and lowest torque ripple. In this respect, researches on current profile shaping and distributed winding configurations are ongoing to improve SR machine performance.

D. PM-ASSISTED SYNCHRONOUS RELUCTANCE MACHINES

The PMaSynR machine derives from the synchronous reluctance (SynR) machine, by inserting PMs into the rotor flux barriers, see Figure 5, to improve the power factor, torque rating and efficiency, with appropriate selection of the PM flux

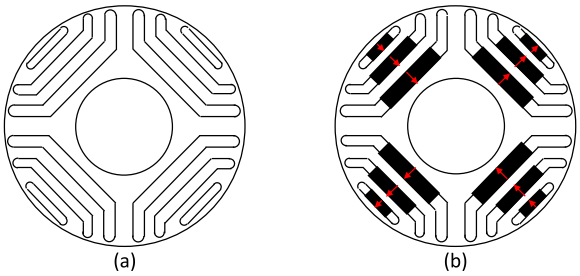

FIGURE 5. Sketches of: (a) SynR rotor, (b) PMaSynR rotor (adapted from [92]).

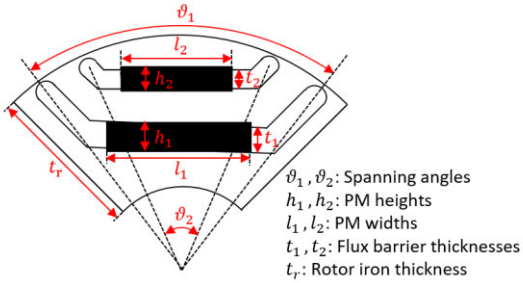

FIGURE 6. Key design parameters in a PMaSynR machine rotor (adapted from [91]).

magnitude [87]–[89]. This machine can also be considered an IPM machine with high saliency and low PM usage, with the advantages of wider speed range at constant power and relatively lower cost. The loss components are similar to those of IPM machines, with the exception of the PM eddy-current loss, which is less significant because of the reduced PM volume.

The rotor geometry plays a key role in restricting the air-gap field harmonics, and thus the torque ripple and iron losses. Reference [90] suggests flux barrier geometries with combined I and U shapes (Figure 5(b)) for future PMaSynR designs, owing to their reduced structural challenges at high speeds, and simpler prototyping. According to [91], the flux barrier spanning angles, defined in Figure 6, are the key parameter to limit the stator iron losses, followed by the PM height. The same study chooses the optimal design of the spanning angles from the minimum loss region of the stator iron loss map as a function of the spanning angles, regardless of the EM operating conditions or PM quantity. The recommendation is for relatively high spanning angles within the specific geometric constraints. At the optimal spanning angles, the iron loss increment with the PM height is limited [91]. In [92], a combined flux barrier structure, called Machaon type, which has two wide barriers and two narrow barriers, is applied to reduce the torque ripple by two thirds with respect to the classic rotor design. Further considerations can be made with respect to the thickness of the flux barriers (see Figure 6). To limit the iron losses while maintaining the torque production capability, the ratio of the total flux barriers thickness, $t_1 + t_2$, to the rotor iron thickness, t_r, is suggested to be slightly higher than that of the stator slot width to the stator slot pitch [93].

The numbers of stator and rotor slots have high impact on both losses and ripple. The rotor slots are realized through the rotor teeth along the airgap surface, which are associated with the flux barriers. In [94], the influence of the stator and rotor slot numbers on torque ripple and iron eddy-current loss in PMaSynR machines is evaluated through an analytical approach based on simplified models of the stator and rotor MMFs. The conclusion is that similar numbers of stator and rotor slots are preferable for minimum iron loss, while a large number of stator slots reduces the torque ripple.

IV. LOSS MINIMIZATION CONTROL METHODS

On an EV, the electric machine needs to output the required torque to drive or brake the vehicle at the current operating speed. Several real-time loss minimization control (LMC) methods have been proposed to maximize EM efficiency for given torque and speed values. These methods can be classified into three categories: i) model based methods, which depend on power loss models, using analytical formulas or look-up tables, and machine parameters; ii) adaptive search methods, based on input power measurement, comparison, and search routines; and iii) methods combining i) and ii).

Various LMC implementations for IM drives covering i)-iii) are summarized in [95], including comparisons in terms of convergence speed, dependence on EM parameters, and accuracy. The results show that model based LMC has the fastest convergence, but the accuracy of the solution highly depends on the machine model and its parameters. Vice versa, search based methods have slow convergence with possible oscillations, but they are not affected by the system parameters.

The selected LMC control variable, x, must have dominant influence on the EM power loss, P_{loss}, and its optimal value is obtained either by solving $\partial P_{loss}/\partial x$, or through an adaptive search routine.

Table 4 summarizes the main LMC variables and power loss models for IMs and PM machines. A simplified PM motor power loss model considering only the copper and iron losses caused by the fundamental current and flux is presented in [96], which specifies the optimal d-axis current, i_d, for power loss minimization through an interval-reduction search algorithm. Compared with the traditional $i_d = 0$ control method, the LMC in [96] improves the efficiency by 3.5% at the rated point. In [97], the optimal d-axis current is obtained by tuning the parameters to achieve minimum input power for each combination of torque and speed. The power loss model in the LMC of [97] includes the stray loss, in addition to the copper and iron losses. In [96], the iron losses are modeled by adding an equivalent core loss resistance, R_c, to the traditional equivalent circuits, whereas in [97] they are based on the empirical formula in Table 4. However,

TABLE 4. Typical power loss formulations and related control variables.

	Power loss model	Ref.	Control variable
IM	$P_{loss} = \left(R_s + \frac{R_c R_r}{R_c + R_r}\right) i_{qs}^2 + \left(R_s + \frac{L_d^2}{R_c + R_r}\omega^2\right) i_{ds}^2$	[98], [100]	i_{ds}, $i_{mr}(i_{qs})$
	$P_{loss} = (R_s + R_r) i_{qs}^2 + \left((\omega L_m)^2 \frac{R_c + R_r}{R_c^2} + R_s\right) i_{ds}^2 - 2\omega L_m \frac{R_r}{R_c} i_{ds} i_{qs}$	[101]	$\lambda_s(i_{ds})$
PM	$P_{loss} = \frac{3}{2} R_s (i_d^2 + i_q^2) + \frac{3}{2}\frac{\omega^2}{R_c}\left[(L_q i_q - L_q i_{cq})^2 + (\lambda_{PM} + L_d i_d - L_d i_{cd})^2\right]$	[96]	i_d
	$P_{loss} = \frac{3}{2} R_s (i_d^2 + i_q^2) + \frac{1}{2} c_{Fe} \omega^\beta L_{md}^2 \left[(i_f + i_d)^2 + \gamma^2 i_q^2\right] + \frac{1}{2} c_{str} \omega^2 (i_d^2 + i_q^2)$	[97]	i_d

Nomenclature. ω: electrical frequency; i_{ds}, i_{qs}: d- and q-axis stator currents of IMs; i_d, i_q, i_{cd}, i_{cq}: d-, q-axis currents and d-, q-axis iron loss currents of PM machines; i_f: equivalent excitation current of PMs; L_d, L_q, L_{md}: d-, q-axis inductances and d-axis magnetizing inductance; L_m: stator and rotor mutual inductance; λ_{PM}: PM flux; c_{Fe}, c_{str}: iron and stray loss coefficients; γ: saliency ratio; β = 1.5~1.6.

in the above studies these LMC methods were only tested and evaluated in steady-state conditions for given operating points.

Although for simplicity the EM parameters are mostly assumed constant in the model based LMC implementations, during real operation their variations with torque, speed and temperature are rather significant in EV applications [98]. The parameter variations are identified from variables such as the load torque, temperature, stator frequency, and voltage [98]. Real-time estimation techniques using the reactive power error, torque error, and an error function based on stator voltage are proposed in [99]. The torque error based method is employed in [101] to estimate the stator and rotor resistances, R_s and R_r, for the LMC model, in which the optimal stator flux (λ_s) for minimum loss is set through volts-per-hertz control. On the other hand, the LMC scheme in [100] employs an online parameter adaptation mechanism to update rotor resistance, and hence to improve the control accuracy of the rotor magnetizing current, i_{mr}. Reference [102] mentions that the EM efficiency can be improved by 0.1% to 0.2% by considering the EM parameter variations with winding and PM temperatures in the model based LMC algorithm.

In terms of LMC results during driving cycles, in [62] the average energy efficiency of an IM under copper loss minimization control is increased by 3% to 6% depending on the cycle, with respect to the rated flux control case. In [102], the efficiency along the NEDC and WLTP achievable through an LMC strategy is compared with that under maximum-torque-per-ampere (MTPA) control, which minimizes the copper loss for an IPM machine. The results show 1% to 2% potential efficiency improvement at low-to-medium torque and medium-to-high speed.

V. DRIVING CYCLE BASED MACHINE OPIMIZATION

Conventional EM design methodologies focus on the rated operating point, especially for applications dominated by steady-state behavior, e.g., pumps and fans. However, in real-life conditions, the operating points of EV machines are mainly far from the rated point, which may cause discrepancy between the high efficiency areas of the torque-speed map and the regions with high operating frequency. Thus, the conventional EM design methods are not the most suitable for EVs; instead, driving cycle based approaches are highly recommended.

In this context, reference [103] deals with the minimization of an IPM motor loss and required machine length for a passenger car over a driving cycle, based on finite element analysis (FEA) coupled with a population based differential evolution algorithm. The results show that "the longer machines with more active material tend to have lower losses in comparison to smaller ones." However, the optimization process is time-consuming due to the multi-objective, high-dimensional and nonlinear problem, with finite element computations of the efficiency map for each candidate design.

To accelerate the optimization routine, an option is to select a limited number of equivalent operating points for EM analysis and evaluation. The concepts of "geometrical center of gravity" [104] and "energy center of gravity" [105] have been introduced for selecting representative operating points from a given driving cycle. In [105], the SPM motor optimized at the rated point has lower copper energy loss but higher iron energy loss than that the machine designed over the representative points, and produces 17% higher motor energy loss along the NEDC. In fact, the power loss contents at the rated point are quite different from those at the representative points. Therefore, the motor design at the rated point focuses on the reduction of copper loss, whereas the motor optimization over the representative points achieves a balance between copper and iron losses over the whole driving schedule. According to [104], the benefit of driving cycle based optimization is negligible for machines operating mostly at low speed (close to the base speed), whereas it is significant for applications with frequent high speed operation.

Another method to reduce the number of FEA computations uses surrogate analytical equations or reluctance networks to derive the power losses and voltage at different torque and speed values. The analytical model and reluctance network model of an SPM machine are proposed and compared in [106], to calculate the EM torque and losses at each operating point, bringing good accuracy and time savings in the optimization process. Reference [107] proposes a fast method to estimate the iron losses along driving cycles, based on the no-load and short-circuit iron loss predicted through FEA. The FEA is performed only once for each iteration, to calculate the base data to derive the iron losses during the driving cycles. The combination of energy weighted operating points and surrogate models is adopted in [108] and [109] for the optimization of SPM and IPM EV motors, showing

fast and stable convergence. An adaptive network based fuzzy inference system that combines the principles of neural networks and fuzzy logic is proposed in [110] to calculate the efficiency map for each candidate EM design. The surrogate models in [109] and [110] reduce the simulation time by up to two orders of magnitude with respect to FEA.

VI. RECENT DEVELOPMENTS

Novel EM technologies for EV powertrains have been proposed to increase operational flexibility, power density, and system efficiency.

A. IN-WHEEL MACHINES

In-wheel motor technology brings significant potential innovations: i) re-arrangement of the EV configuration by placing the EMs adjacent to or inside the wheels [111], see Figure 7, rather than on-board. The in-wheel arrangement significantly reduces the chassis volume required by the powertrain components, and increases the space available for the EV occupants. The motor is designed with large diameter and short axial length to fit inside the wheel, and an outer rotor topology is preferred for direct drive applications; ii) continuous and seamless generation of direct yaw moments through different wheel torque levels on the two EV sides, to improve cornering response and active safety, by using controllers like those in [112]; and iii) enhanced wheel torque generation accuracy, especially during extreme transients, such as those associated with the interventions of the anti-lock braking system (ABS) and traction control [113]. The superior wheel torque control bandwidth of in-wheel powertrains is caused by the absence of the torsional dynamics of the half-shafts and constant velocity joints, and can result in reduced stopping distances and acceleration times [111].

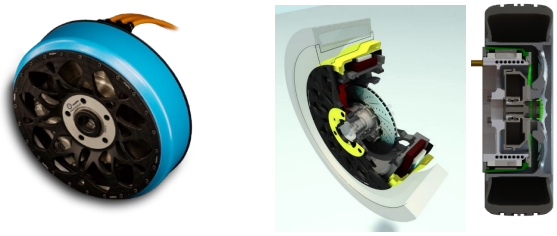

FIGURE 7. Examples of in-wheel motor arrangements. (a) Elaphe L1500 unit, (b) Wheel assembly with direct drive in-wheel unit (courtesy of Elaphe).

Past academic studies suggest combining in-wheel technology with PM and SR machines [114], [115]. Currently, there are available in-wheel powertrains developed by automotive technology firms, such as: i) Elaphe, Protean, QS Motor, and Schaeffler, offering PM direct drive machines (see Table 3); and ii) ECOmove and NTN, proposing near-the-wheel layouts with a PM machine and a mechanical transmission [116], [117]. However, all of them have yet to be extensively used in production EVs.

The in-wheel powertrain efficiency is potentially improved by the elimination of the mechanical transmission in direct drive configurations [118], and appropriate wheel torque distribution techniques during EV operation; however, the low-speed high-torque direct drive EMs tend to be less efficient than conventional high-speed low-torque on-board traction motors. The literature misses a systematic efficiency-oriented comparison of in-wheel and on-board powertrain solutions. In this respect, preliminary results are reported in [119]. More comprehensive analyses are being carried out in ongoing research projects, such as the H2020 European project EVC1000 [120]. Challenges in the in-wheel powertrain technology remain with respect to the demanding requirements in terms of torque/power density, safety and reliability, as well as suspension and wheel assembly design [111].

B. NOVEL MACHINE TOPOLOGIES

In recent decades, several EM topologies have been proposed for EVs, including stator PM, flux memory, hybrid excitation, multiphase, magnetic geared and reconfigurable winding machines [121].

1) STATOR PM MACHINES

With the PMs installed in the stator, stator PM machines inherit some of the merits of both PM synchronous machines and SR machines, and also overcome the PM cooling problems of rotor PM machines. The side effects are: i) the ease of saturation of the stator iron teeth, which limits the motor overload capability [122]; and ii) the fact that these machines cannot maintain high efficiency over a wide speed range, because of the uncontrollable PM flux.

2) FLUX MEMORY MACHINES AND HYBRID EXCITATION MACHINES

To overcome the flux weakening restrictions owing to the fixed PM excitation in PM machines, flux memory machines and hybrid excitation machines are proposed by applying PMs with relatively low coercive force (such as AlNiCo magnets) and field windings, respectively, to realize on-line flux adjustment. Since less negative d-axis current is required, an efficiency improvement can be expected in these types of machines, especially in the high-speed region [123].

3) MULTIPHASE MACHINES

Multiphase machines have drawn wide attention due to their intrinsic features such as power splitting, better fault-tolerance and lower torque ripple than three-phase machines. Recent advances in the machine topology, modeling and control aspects of multiphase drives for automotive traction applications are reviewed in [124], where the six-phase drives are extensively covered. As discussed in [125], the motor and converter efficiencies in three-phase and six-phase drives are very close in high frequency applications. However, it is also indicated that an efficiency advantage of six-phase machines can be expected in situations in which the copper loss is much larger than the iron loss. In multiphase EV drives, the overall

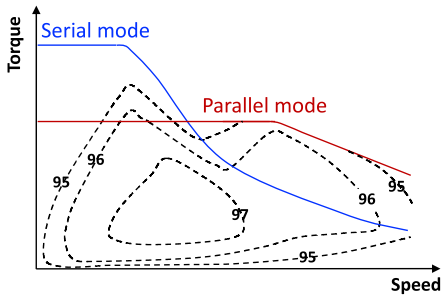

FIGURE 8. Combined motor efficiency plot for serial and parallel modes (adapted from [22]).

converter and motor efficiency can be enhanced by appropriate selection of the number of active converter legs, according to the load and speed conditions [126]. However, cost and system reliability should be carefully evaluated, given the increased complexity of the power electronic devices.

4) MAGNETIC GEARED MACHINES

Magnetic geared machines have been proposed to achieve low-speed high-torque operation based on the magnetic gearing effect, which is very desirable for direct drive applications. Different topologies have been investigated for EVs and HEVs, such as in-wheel magnetic geared PM machines [127], Vernier machines [128] and magnetic geared dual-rotor machines [129]. Their operation principle has been unified by the general field modulation theory [130], which also provides guidance for inventing new machine topologies. Although [127] states that such machines have good efficiency and power density characteristics, an objective energy efficiency comparison with other machine topologies is currently missing, to the best of our knowledge.

5) RECONFIGURABLE WINDING MACHINES

Reconfigurable windings were originally developed to achieve faster motor start-up in IMs [131]. However, they can also be adopted in PM machines to expand the premium efficiency region by switching the winding configuration from serial mode, suitable for low-speed and high-torque operation, to parallel mode, more efficient for high-speed and high-power operation, see Figure 8 [22]. The switching algorithm can be based on the efficiency values provided by each configuration. The study in [22] evaluates the efficiency impact of reconfigurable windings on an IPM machine similar to the 2010 Toyota Prius motor. On this topic, recent advances have been made on reconfiguration systems using fewer active switches [132]. The main challenges of reconfigurable winding technology are the practical implementation and cost of the additional switches, as well as the complex machine geometries and assemblies [131].

VII. CONCLUSION

This literature review discussed design approaches and control methods for EV traction machines, with focus on the efficiency enhancement over realistic EV mission profiles. The following aspects were highlighted:

- The centralized on-board powertrain layout remains the mainstream for electric cars, and is adopted in two-wheel-drive and all-wheel-drive EVs, where the latter provide better traction and handling performance, particularly desirable in premium passenger cars. An increasing number of AWD EVs have different EM designs on the two axles, to achieve the best compromise in terms of efficiency, performance, and cost.
- The general recent trend in EV motor topologies is toward the adoption of PM synchronous machines with reduced rare-earth PM material content. In this context, PMaSynR machines represent an attractive option.
- The main roadmap specifications for future EV machines target significant power density increments and important cost reductions. The expected efficiency increase is minor or major, depending on the considered roadmap.
- Similar and relatively large numbers of stator and rotor slots are preferable for low harmonic losses and torque ripple. The rotor geometries are of great importance to limit the harmonic losses. The main relevant characteristics are the rotor slot shapes for IMs, PM arrangements for IPM machines, and spanning angles of the rotor barriers for PMaSynR machines.
- From the control viewpoint, LMC strategies enable the motor to operate at its highest efficiency for each torque and speed condition. The LMC scheme for a specific application should be selected as a trade-off between desired convergence speed, parameter sensitivity and convergence error.
- Driving cycle based motor design and optimization approaches are essential to meet the energy efficiency requirements of modern EVs. Significant work is ongoing to reduce the computational burden of these routines, while maintaining high accuracy of the solution.
- In-wheel motor layouts offer significant benefits in terms of vehicle design and performance, at the price of increased complexity of the wheel hub assembly. A systematic efficiency comparison between in-wheel and on-board powertrain layouts is currently missing from the available literature.
- Novel EM topologies, namely stator PM, flux memory, hybrid excitation, multiphase, magnetic geared and reconfigurable winding machines, are potentially efficient candidates for EV powertrains.

REFERENCES

[1] K. Rajashekara, "Present status and future trends in electric vehicle propulsion technologies," *IEEE J. Emerg. Sel. Topics Power Electron.*, vol. 1, no. 1, pp. 3–10, Mar. 2013.

[2] J. de Santiago, H. Bernhoff, B. Ekergård, S. Eriksson, S. Ferhatovic, R. Waters, and M. Leijon, "Electrical motor drivelines in commercial all-electric vehicles: A review," *IEEE Trans. Veh. Technol.*, vol. 61, no. 2, pp. 475–484, Feb. 2012.

[3] (Mar. 2020). *Driving the Future of HEV/EV with High-Voltage Solutions*. [Online]. Available: https://www.powerelectronics.com/markets/automotive/article/21864063/driving-the-future-of-hevev-with-highvoltage-solutions
[4] H. M. Fischer and L. Dorn, *Voltage Classes for Electric Mobility*. Frankfurt, Germany: ZVEI—German Electrical and Electronic Manufacturers' Association, Centre of Excellence Electric Mobility, Dec. 2013.
[5] T. Burress and S. Campbell, "Benchmarking EV and HEV power electronics and electric machines," in *Proc. IEEE Transp. Electrific. Conf. Expo (ITEC)*, Jun. 2013, pp. 1–6.
[6] K. Mueller and R. Heinrich, "Modern high voltage drive train architecture to accommodate the needs for a variety of components for future automotive applications," in *Proc. Conf. Future Automot. Technol., Focus Electromobility*, Munchen, Germany, Mar. 2013, pp. 1–8.
[7] A. Stippich, C. H. Van Der Broeck, and A. Sewergin, "Key components of modular propulsion systems for next generation electric vehicles," *CPSS Trans. Power Electron. Appl.*, vol. 2, no. 4, pp. 249–258, Dec. 2017.
[8] A. Emadi, S. S. Williamson, and A. Khaligh, "Power electronics intensive solutions for advanced electric, hybrid electric, and fuel cell vehicular power systems," *IEEE Trans. Power Electron.*, vol. 21, no. 3, pp. 567–577, May 2006.
[9] (Jun. 2020). *Global EV Sales*. [Online]. Available: http://www.ev-volumes.com/country/total-world-plug-in-vehicle-volumes/
[10] (Sep. 2019). *Press Information The Audi e-Tron*. [Online]. Available: https://www.audi-mediacenter.com
[11] (Sep. 2019). *All-electric Jaguar I-Pace*. [Online]. Available: https://www.jaguar.co.uk/Images/Jaguar-I-PACE-Brochure-1X5901910000BGBEN01P_tcm634-609064.pdf
[12] (Sep. 2019). *Tesla Model 3 Dual Motor and Performance Versions Get Official EPA Ratings*. [Online]. Available: https://electrek.co/2018/07/17/tesla-model-3-dual-motor-performance-versions-official-epa-ratings/
[13] (Sep. 2019). *Tesla's Top Motor Engineer Talks About Designing a Permanent Magnet Machine for Model 3*. [Online]. Available: https://chargedevs.com/features/teslas-top-motor-engineer-talks-about-designing-a-permanent-magnet-machine-for-model-3/
[14] Z. Q. Zhu, W. Q. Chu, and Y. Guan, "Quantitative comparison of electromagnetic performance of electrical machines for HEVs/EVs," *CES Trans. Elec. Mach. Syst.*, vol. 1, no. 1, pp. 37–47, Mar. 2017.
[15] G. Pellegrino, A. Vagati, B. Boazzo, and P. Guglielmi, "Comparison of induction and PM synchronous motor drives for EV application including design examples," *IEEE Trans. Ind. Appl.*, vol. 48, no. 6, pp. 2322–2332, Nov. 2012.
[16] B. Sarlioglu, C. T. Morris, D. Han, and S. Li, "Driving toward accessibility: A review of technological improvements for electric machines, power electronics, and batteries for electric and hybrid vehicles," *IEEE Ind. Appl. Mag.*, vol. 23, no. 1, pp. 14–25, Jan. 2017.
[17] G. Pellegrino, A. Vagati, P. Guglielmi, and B. Boazzo, "Performance comparison between surface-mounted and interior PM motor drives for electric vehicle application," *IEEE Trans. Ind. Electron.*, vol. 59, no. 2, pp. 803–811, Feb. 2012.
[18] Z. Yang, F. Shang, I. P. Brown, and M. Krishnamurthy, "Comparative study of interior permanent magnet, induction, and switched reluctance motor drives for EV and HEV applications," *IEEE Trans. Transport. Electrific.*, vol. 1, no. 3, pp. 245–254, Oct. 2015.
[19] R. H. Staunton, T. A. Burress, and L. D. Marlino, "Evaluation of 2005 Honda Accord hybrid electric drive system," Oak Ridge Nat. Lab., Oak Ridge, TN, USA, Tech. Rep. TM-2006-535, Sep. 2006.
[20] T. A. Burress, S. L. Campbell, and C. Coomer, "Evaluation of the 2010 Toyota Prius hybrid synergy drive system," Oak Ridge Nat. Lab., Oak Ridge, TN, USA, Tech. Rep. TM-2010-253, Mar. 2011.
[21] Y. Sato, S. Ishikawa, and T. Okubo, "Development of high response motor and inverter system for the Nissan LEAF electric vehicle," SAE Tech. Paper 2011-01-0350, Apr. 2011.
[22] *U.S. Dept. Energy, FY 2016 Annual Progress Report for Electric Drive Technologies Program*, document DOE/EE-1532, Annual Progress Report, Jul. 2017.
[23] P. Ramesh and N. C. Lenin, "High power density electrical machines for electric vehicles–comprehensive review based on material technology," *IEEE Trans. Magn.*, vol. 55, no. 11, pp. 1–21, Nov. 2019.
[24] (Jan. 2020). *What is Ziptron*. [Online]. Available: https://ev.tatamotors.com/technology/
[25] (Jan. 2020). *Newest Electric Vehicles*. [Online]. Available: https://ev-database.org/compare/newest-upcoming-electric-vehicle
[26] (Jan. 2020). *MG ZS EV*. [Online]. Available: https://mg.co.uk/mg-zs-electric/specifications/
[27] (Jan. 2020). *Chinese Cars*. [Online]. Available: http://www.chinamobil.ru/eng/
[28] (Jan. 2020). *EX3*. [Online]. Available: https://www.bjev.com.cn/html/ex3.html
[29] (Jan. 2020). *JAC iEV*. [Online]. Available: https://www.jac.com.cn/jacweb/iev/
[30] (Sep. 2019). *Smart EQ Fortwo and Forfour*. [Online]. Available: https://tools.mercedes-benz.co.uk/current/smart/pricelists/smart-electric-drive.pdf
[31] (Jan. 2020). *EQC*. [Online]. Available: http://tools.mercedes-benz.co.uk/current/passenger-cars/e-brochures/eqc.pdf?owda=misc
[32] (Sep. 2019). *Kia Niro EV Specifications*. Accessed: 2019. [Online]. Available: https://www.kiamedia.com/us/en/models/niro-ev/2019/
[33] (Jan. 2020). *All-New Hyundai Kona Electric—Technical Data and Dimensions*. [Online]. Available: https://www.hyundai.news/eu/press-kits/all-new-hyundai-kona-electric-technical-data-and-dimensions/
[34] (Sep. 2019). *BAIC BJEV Profile*. [Online]. Available: https://www.kcci.kharkov.ua/upload/files/BAIC%20BJEV%20Profile%20201702.pdf
[35] (Sep. 2019). *Model S: Premium Electric Sedan*. [Online]. Available: https://www.tesla.com/sites/default/files/tesla-model-s.pdf
[36] (Sep. 2019). *BMW_i3_Brochure*. [Online]. Available: https://www.bmw.co.uk/pdfs/brochures/BMW_i3_Brochure_June19.pdf
[37] (Sep. 2019). *Compare ZOE*. [Online]. Available: https://www.renault.co.uk/vehicles/new-vehicles/zoe/compare.html
[38] (Sep. 2019). *Fiat 500e*. [Online]. Available: https://www.topspeed.com/cars/fiat/2019-fiat-500e-ar183749.html
[39] (Sep. 2019). *Mercedes-Benz SLS AMG Coupé Electric Drive*. [Online]. Available: https://media.daimler.com/marsMediaSite
[40] (Sep. 2019). *Tesla Motors—Acceleration and Torque*. [Online]. Available: https://web.archive.org/web/20071017141420/http://www.teslamotors.com/performance/
[41] Electric Machines Roadmap. *Advanced Propulsion Centre in Collaboration With Automotive Council, UK*. [Online]. Available: https://www.apcuk.co.uk/app/uploads/2018/02/EMC_Full_Pack.pdf
[42] Electrical and Electronics Technical Team Roadmap. (Oct. 2017). *U.S. DRIVE Partnership, US*. [Online]. Available: https://www.energy.gov/sites/prod/files/2017/11/f39/EETT%20Roadmap%2010-27-17.pdf
[43] A. M. EL-Refaie, J. P. Alexander, S. Galioto, P. B. Reddy, K.-K. Huh, P. de Bock, and X. Shen, "Advanced high-power-density interior permanent magnet motor for traction applications," *IEEE Trans. Ind. Appl.*, vol. 50, no. 5, pp. 3235–3248, Oct. 2014.
[44] (Sep. 2019). *What is WLTP and How Does it Work?*. [Online]. Available: https://wltpfacts.eu/what-is-wltp-how-will-it-work/
[45] *European Roadmap Electrification of Road Transport*, 3rd ed, ERTRAC, EPoSS and ETIP SNET, Brussels, Belgium, Jun. 2017.
[46] M. Cheng and M. Tong, "Development status and trend of electric vehicles in China," *Chin. J. Electr. Eng.*, vol. 3, no. 2, pp. 1–13, Sep. 2017.
[47] (Sep. 2019). *EP2*. [Online]. Available: https://www.punchpowertrain.com/en/products/23/ep2
[48] (Sep. 2019). *E-Motor 120kW / 130Nm*. [Online]. Available: https://www.mclaren.com/appliedtechnologies/products/item/e-motor-120kw-130nm/
[49] (Sep. 2019). *Drive Components for Hybrid and Electric Vehicles—SIVETEC*. [Online]. Available: https://w3.siemens.com/topics/global/en/electromobility/pages/powertrain-ecar.aspx
[50] (Sep. 2019). *Powertrain Electrification Separate Motor Generator (SMG)*. [Online]. Available: http://life.bosch.com.cn/ebrochures2015/energizing_powertrain/E_BROCHURE_UAES/Permanent_Mobility_With_Electrical_Drives_and_Hybrid_Technology/Separate_Motor_Generator.pdf
[51] (Sep. 2019). *JJE 140kW Motor OD220*. [Online]. Available: http://www.jjecn.com/?c=show&m=view&id=7
[52] (Sep. 2019). *New Energy E-Drive System*. [Online]. Available: http://www.jee-china.com/info_60.aspx-itemid=238.htm
[53] (Sep. 2019). *YASA P400 R Series E-Motors*. [Online]. Available: https://www.yasa.com/wp-content/uploads/2018/01/YASA_P400_Product_Sheet.pdf
[54] (Sep. 2019). *Zytek Integrated 55kW Electric Engine*. [Online]. Available: http://www.zytekautomotive.co.uk/products/electric-engines/55kw/
[55] (Sep. 2019). *TM4 MOTIVE, Redefined*. [Online]. Available: https://www.danatm4.com/products/motive-high-speed-electric-powertrain/

[56] (Sep. 2019). *Pd18 Datasheet*. [Online]. Available: https://www.proteanelectric.com/f/2018/05/Pd18-Datasheet-Master.pdf

[57] (Sep. 2019). *Elaphe L1500 Ver. D*. [Online]. Available: https://in-wheel.com/media/website/059_L1500D_Technical_Specification_Preliminary-compressed.pdf

[58] Y. Gai, M. Kimiabeigi, Y. Chuan Chong, J. D. Widmer, X. Deng, M. Popescu, J. Goss, D. A. Staton, and A. Steven, "Cooling of automotive traction motors: Schemes, examples, and computation methods," *IEEE Trans. Ind. Electron.*, vol. 66, no. 3, pp. 1681–1692, Mar. 2019.

[59] E. Hendrickson, "Optimize your vehicle by cooling electric motors and generators," *Mech. Motion Syst.*, Nov. 2017. [Online]. Available: https://www.machinedesign.com/mechanical-motion-systems/article/21836174/optimize-your-vehicle-by-cooling-electric-motors-and-generators

[60] M. K. Yoon, C. S. Jeon, and S. Ken Kauh, "Efficiency increase of an induction motor by improving cooling performance," *IEEE Trans. Energy Convers.*, vol. 17, no. 1, pp. 1–6, Mar. 2002.

[61] S. Williamson, M. Lukic, and A. Emadi, "Comprehensive drive train efficiency analysis of hybrid electric and fuel cell vehicles based on motor-controller efficiency modeling," *IEEE Trans. Power Electron.*, vol. 21, no. 3, pp. 730–740, May 2006.

[62] V. T. Buyukdegirmenci, A. M. Bazzi, and P. T. Krein, "Evaluation of induction and permanent-magnet synchronous machines using drive-cycle energy and loss minimization in traction applications," *IEEE Trans. Ind. Appl.*, vol. 50, no. 1, pp. 395–403, Jan. 2014.

[63] T. Wang, P. Zheng, Q. Zhang, and S. Cheng, "Design characteristics of the induction motor used for hybrid electric vehicle," *IEEE Trans. Magn.*, vol. 41, no. 1, pp. 505–508, Jan. 2005.

[64] Z. M. Zhao, S. Meng, C. C. Chan, and E. W. C. Lo, "A novel induction machine design suitable for inverter-driven variable speed systems," *IEEE Trans. Energy Convers.*, vol. 15, no. 4, pp. 413–420, Dec. 2000.

[65] Q. Zhang, H. Liu, Z. Zhang, and T. Song, "A cast copper rotor induction motor for small commercial EV traction: Electromagnetic design, analysis, and experimental tests," *China Electrotech. Soc. Trans. Electr. Mach. Syst.*, vol. 2, no. 4, pp. 417–424, Dec. 2018.

[66] J. Malinowski, J. McCormick, and K. Dunn, "Advances in construction techniques of AC induction motors: Preparation for super-premium efficiency levels," *IEEE Trans. Ind. Appl.*, vol. 40, no. 6, pp. 1665–1670, Nov. 2004.

[67] K. Yamazaki and H. Ishigami, "Rotor-shape optimization of Interior-Permanent-Magnet motors to reduce harmonic iron losses," *IEEE Trans. Ind. Electron.*, vol. 57, no. 1, pp. 61–69, Jan. 2010.

[68] N. Bianchi, S. Bolognani, and E. Fornasiero, "An overview of rotor losses determination in three-phase fractional-slot PM machines," *IEEE Trans. Ind. Appl.*, vol. 46, no. 6, pp. 2338–2345, Nov. 2010.

[69] J. Wang, X. Yuan, and K. Atallah, "Design optimization of a surface-mounted permanent-magnet motor with concentrated windings for electric vehicle applications," *IEEE Trans. Veh. Technol.*, vol. 62, no. 3, pp. 1053–1064, Mar. 2013.

[70] K. M. Rahman, S. Jurkovic, C. Stancu, J. Morgante, and P. J. Savagian, "Design and performance of electrical propulsion system of extended range electric vehicle (EREV) chevrolet volt," *IEEE Trans. Ind. Appl.*, vol. 51, no. 3, pp. 2479–2488, May 2015.

[71] X. Fan, B. Zhang, R. Qu, D. Li, J. Li, and Y. Huo, "Comparative thermal analysis of IPMSMs with integral-slot distributed-winding (ISDW) and fractional-slot concentrated-winding (FSCW) for electric vehicle application," *IEEE Trans. Ind. Appl.*, vol. 55, no. 4, pp. 3577–3588, Jul. 2019.

[72] G. Berardi and N. Bianchi, "Design guideline of an AC hairpin winding," in *Proc. 8th Int. Conf. Electr. Mach. (ICEM)*, Sep. 2018, pp. 2444–2450.

[73] X. Liu, H. Chen, J. Zhao, and A. Belahcen, "Research on the performances and parameters of interior PMSM used for electric vehicles," *IEEE Trans. Ind. Electron.*, vol. 63, no. 6, pp. 3533–3545, Jun. 2016.

[74] S. Chowdhury, E. Gurpinar, G.-J. Su, T. Raminosoa, T. A. Burress, and B. Ozpineci, "Enabling technologies for compact integrated electric drives for automotive traction applications," in *Proc. IEEE Transp. Electrific. Conf. Expo (ITEC)*, Jun. 2019, pp. 1–8.

[75] Y. Yang, S. M. Castano, R. Yang, M. Kasprzak, B. Bilgin, A. Sathyan, H. Dadkhah, and A. Emadi, "Design and comparison of interior permanent magnet motor topologies for traction applications," *IEEE Trans. Transport. Electrific.*, vol. 3, no. 1, pp. 86–97, Mar. 2017.

[76] E. Sayed, Y. Yang, B. Bilgin, M. H. Bakr, and A. Emadi, "A comprehensive review of flux barriers in interior permanent magnet synchronous machines," *IEEE Access*, vol. 7, pp. 149168–149181, Oct. 2019.

[77] W. Zhao, F. Zhao, T. A. Lipo, and B.-I. Kwon, "Optimal design of a novel V-Type interior permanent magnet motor with assisted barriers for the improvement of torque characteristics," *IEEE Trans. Magn.*, vol. 50, no. 11, Nov. 2014, Art. no. 8104504.

[78] K. Yamazaki, Y. Kato, T. Ikemi, and S. Ohki, "Reduction of rotor losses in multilayer interior permanent-magnet synchronous motors by introducing novel topology of rotor flux barriers," *IEEE Trans. Ind. Appl.*, vol. 50, no. 5, pp. 3185–3193, Oct. 2014.

[79] E. Carraro and N. Bianchi, "Design and comparison of interior permanent magnet synchronous motors with non-uniform airgap and conventional rotor for electric vehicle applications," *IET Electr. Power Appl.*, vol. 8, no. 6, pp. 240–249, Jul. 2014.

[80] M. Besharati, J. Widmer, G. Atkinson, V. Pickert, and J. Washington, "Super-high-speed switched reluctance motor for automotive traction," in *Proc. IEEE Energy Convers. Congr. Exposit. (ECCE)*, Sep. 2015, pp. 5241–5248.

[81] K. M. Rahman, B. Fahimi, G. Suresh, A. V. Rajarathnam, and M. Ehsani, "Advantages of switched reluctance motor applications to EV and HEV: Design and control issues," *IEEE Trans. Ind. Appl.*, vol. 36, no. 1, pp. 111–121, Jan. 2000.

[82] C. Gan, J. Wu, Q. Sun, W. Kong, H. Li, and Y. Hu, "A review on machine topologies and control techniques for low-noise switched reluctance motors in electric vehicle applications," *IEEE Access*, vol. 6, pp. 31430–31443, 2018.

[83] E. Bostanci, M. Moallem, A. Parsapour, and B. Fahimi, "Opportunities and challenges of switched reluctance motor drives for electric propulsion: A comparative study," *IEEE Trans. Transport. Electrific.*, vol. 3, no. 1, pp. 58–75, Mar. 2017.

[84] P. Azer, B. Bilgin, and A. Emadi, "Mutually coupled switched reluctance motor: Fundamentals, control, modeling, state of the art review and future trends," *IEEE Access*, vol. 7, pp. 100099–100112, 2019.

[85] K. Kiyota, T. Kakishima, and A. Chiba, "Comparison of test result and design stage prediction of switched reluctance motor competitive with 60-kW rare-Earth PM motor," *IEEE Trans. Ind. Electron.*, vol. 61, no. 10, pp. 5712–5721, Oct. 2014.

[86] K. M. Rahman and S. E. Schulz, "Design of high-efficiency and high-torque-density switched reluctance motor for vehicle propulsion," *IEEE Trans. Ind. Appl.*, vol. 38, no. 6, pp. 1500–1507, Nov. 2002.

[87] S. Morimoto, M. Sanada, and Y. Takeda, "Performance of PM assisted synchronous reluctance motor for high efficiency and wide constant power operation," in *Proc. Conf. Rec. IEEE Ind. Appl. Conf. 25th IAS Annu. Meeting World Conf. Ind. Appl. Electr. Energy*, Oct. 2000, pp. 1–6.

[88] T. Mohanarajah, M. Nagrial, J. Rizk, and A. Hellany, "Permanent magnet optimization in PM assisted synchronous reluctance machines," in *Proc. IEEE 27th Int. Symp. Ind. Electron. (ISIE)*, Jun. 2018, pp. 1347–1351.

[89] N. Bianchi, E. Fornasiero, and W. Soong, "Selection of PM flux linkage for maximum low-speed torque rating in a PM-assisted synchronous reluctance machine," *IEEE Trans. Ind. Appl.*, vol. 51, no. 5, pp. 3600–3608, Sep. 2015.

[90] G. Pellegrino, F. Cupertino, and C. Gerada, "Automatic design of synchronous reluctance motors focusing on barrier shape optimization," *IEEE Trans. Ind. Appl.*, vol. 51, no. 2, pp. 1465–1474, Mar. 2015.

[91] M. Barcaro, N. Bianchi, and F. Magnussen, "Rotor flux-barrier geometry design to reduce stator iron losses in synchronous IPM motors under FW operations," *IEEE Trans. Ind. Appl.*, vol. 46, no. 5, pp. 1950–1958, Sep. 2010.

[92] N. Bianchi, S. Bolognani, D. Bon, and M. D. Pre, "Rotor flux-barrier design for torque ripple reduction in synchronous reluctance and PM-assisted synchronous reluctance motors," *IEEE Trans. Ind. Appl.*, vol. 45, no. 3, pp. 921–928, May 2009.

[93] M. Ferrari, N. Bianchi, and E. Fornasiero, "Analysis of rotor saturation in synchronous reluctance and PM-assisted reluctance motors," *IEEE Trans. Ind. Appl.*, vol. 51, no. 1, pp. 169–177, Jan. 2015.

[94] G. Pellegrino, P. Guglielmi, A. Vagati, and F. Villata, "Core loss and torque ripple in IPM machines: Dedicated modeling and design trade off," *IEEE Trans. Ind. Appl.*, vol. 46, no. 6, pp. 2381–2391, Nov./Dec. 2010.

[95] A. M. Bazzi and P. T. Krein, "Review of methods for real-time loss minimization in induction machines," *IEEE Trans. Ind. Appl.*, vol. 46, no. 6, pp. 2319–2328, Nov. 2010.

[96] C. Cavallaro, A. O. Di Tommaso, R. Miceli, A. Raciti, G. R. Galluzzo, and M. Trapanese, "Efficiency enhancement of permanent-magnet synchronous motor drives by online loss minimization approaches," *IEEE Trans. Ind. Electron.*, vol. 52, no. 4, pp. 1153–1160, Aug. 2005.

[97] C. Mademlis, I. Kioskeridis, and N. Margaris, "Optimal efficiency control strategy for interior permanent-magnet synchronous motor drives," *IEEE Trans. Energy Convers.*, vol. 19, no. 4, pp. 715–723, Dec. 2004.
[98] T. Stefanski and S. Karys, "Loss minimisation control of induction motor drive for electrical vehicle," in *Proc. IEEE Int. Symp. Ind. Electron.*, Jun. 1996, pp. 952–957.
[99] J. Faiz and M. B. B. Sharifian, "Different techniques for real time estimation of an induction motor rotor resistance in sensorless direct torque control for electric vehicle," *IEEE Trans. Energy Convers.*, vol. 16, no. 1, pp. 104–109, Mar. 2001.
[100] M. N. Uddin and S. W. Nam, "Development of a nonlinear and model-based online loss minimization control of an IM drive," *IEEE Trans. Energy Convers.*, vol. 23, no. 4, pp. 1015–1024, Dec. 2008.
[101] A. Haddoun, M. E. H. Benbouzid, D. Diallo, R. Abdessemed, J. Ghouili, and K. Srairi, "A loss-minimization DTC scheme for EV induction motors," *IEEE Trans. Veh. Technol.*, vol. 56, no. 1, pp. 81–88, Jan. 2007.
[102] W. Peters, O. Wallscheid, and J. Bocker, "Optimum efficiency control of interior permanent magnet synchronous motors in drive trains of electric and hybrid vehicles," in *Proc. 17th Eur. Conf. Power Electron. Appl. (EPE ECCE-Europe)*, Sep. 2015, pp. 1–10.
[103] S. Gunther, S. Ulbrich, and W. Hofmann, "Driving cycle-based design optimization of interior permanent magnet synchronous motor drives for electric vehicle application," in *Proc. Int. Symp. Power Electron., Electr. Drives, Autom. Motion (SPEEDAM)*, Jun. 2014, pp. 25–30.
[104] E. Carraro, M. Morandin, and N. Bianchi, "Traction PMASR motor optimization according to a given driving cycle," *IEEE Trans. Ind. Appl.*, vol. 52, no. 1, pp. 209–216, Jan. 2016.
[105] P. Lazari, J. Wang, and L. Chen, "A computationally efficient design technique for electric-vehicle traction machines," *IEEE Trans. Ind. Appl.*, vol. 50, no. 5, pp. 3203–3213, Sep. 2014.
[106] L. Dang, N. Bernard, N. Bracikowski, and G. Berthiau, "Design optimization with flux weakening of high-speed PMSM for electrical vehicle considering the driving cycle," *IEEE Trans. Ind. Electron.*, vol. 64, no. 12, pp. 9834–9843, Dec. 2017.
[107] V. Ruuskanen, J. Nerg, M. Rilla, and J. Pyrhonen, "Iron loss analysis of the permanent-magnet synchronous machine based on finite-element analysis over the electrical vehicle drive cycle," *IEEE Trans. Ind. Electron.*, vol. 63, no. 7, pp. 4129–4136, Jul. 2016.
[108] A. G. Sarigiannidis, M. E. Beniakar, and A. G. Kladas, "Fast adaptive evolutionary PM traction motor optimization based on electric vehicle drive cycle," *IEEE Trans. Veh. Technol.*, vol. 66, no. 7, pp. 5762–5774, Jul. 2017.
[109] A. Fatemi, N. A. O. Demerdash, T. W. Nehl, and D. M. Ionel, "Large-scale design optimization of PM machines over a target operating cycle," *IEEE Trans. Ind. Appl.*, vol. 52, no. 5, pp. 3772–3782, Sep. 2016.
[110] C. T. Krasopoulos, M. E. Beniakar, and A. G. Kladas, "Multicriteria PM motor design based on ANFIS evaluation of EV driving cycle efficiency," *IEEE Trans. Transport. Electrific.*, vol. 4, no. 2, pp. 525–535, Jun. 2018.
[111] S. Murata, "Innovation by in-wheel-motor drive unit," *Vehicle Syst. Dyn.*, vol. 50, no. 6, pp. 807–830, Jun. 2012.
[112] L. De Novellis, A. Sorniotti, P. Gruber, J. Orus, J.-M. R. Fortun, J. Theunissen, and J. De Smet, "Direct yaw moment control actuated through electric drivetrains and friction brakes: Theoretical design and experimental assessment," *Mechatronics*, vol. 26, pp. 1–15, Mar. 2015.
[113] D. Tavernini, M. Metzler, P. Gruber, and A. Sorniotti, "Explicit nonlinear model predictive control for electric vehicle traction control," *IEEE Trans. Control Syst. Technol.*, vol. 27, no. 4, pp. 1438–1451, Jul. 2019.
[114] J. Wang, K. Atallah, Z. Q. Zhu, and D. Howe, "Modular three-phase permanent-magnet brushless machines for in-wheel applications," *IEEE Trans. Veh. Technol.*, vol. 57, no. 5, pp. 2714–2720, Sep. 2008.
[115] X. D. Xue, K. W. E. Cheng, T. W. Ng, and N. C. Cheung, "Multi-objective optimization design of in-wheel switched reluctance motors in electric vehicles," *IEEE Trans. Ind. Electron.*, vol. 57, no. 9, pp. 2980–2987, Sep. 2010.
[116] (Oct. 2019). *ECOMOVE Electric Powertrain*. [Online]. Available: http://ecomove.dk/wp-content/uploads/2013/06/ECOmove-Powertrain-Specifications.pdf
[117] (Sep. 2019). *NTN News 2012*. [Online]. Available: https://www.ntnglobal.com/en/news/press/news201200066.html
[118] M. Terashima, T. Ashikaga, T. Mizuno, K. Natori, N. Fujiwara, and M. Yada, "Novel motors and controllers for high-performance electric vehicle with four in-wheel motors," *IEEE Trans. Ind. Electron.*, vol. 44, no. 1, pp. 28–38, Feb. 1997.
[119] A. Watts, A. Vallance, and A. Whitehead, "The technology and economics of in-wheel motors," *SAE Int. J. Passeng. Cars-Electron. Elect. Syst.*, vol. 3, no. 2, pp. 37–57, Oct. 2010.
[120] (Oct. 2019). *Electric Vehicle Components for 1000 Km Daily Trips (EVC1000)*. [Online]. Available: http://www.evc1000.eu/en/
[121] M. Cheng, L. Sun, G. Buja, and L. Song, "Advanced electrical machines and machine-based systems for electric and hybrid vehicles," *Energies*, vol. 8, no. 9, pp. 9541–9564, Sep. 2015.
[122] M. Cheng, W. Hua, J. Zhang, and W. Zhao, "Overview of stator-permanent magnet brushless machines," *IEEE Trans. Ind. Electron.*, vol. 58, no. 11, pp. 5087–5101, Nov. 2011.
[123] X. Liu, D. Wu, Z. Q. Zhu, A. Pride, R. P. Deodhar, and T. Sasaki, "Efficiency improvement of switched flux PM memory machine over interior PM machine for EV/HEV applications," *IEEE Trans. Magn.*, vol. 50, no. 11, pp. 1–4, Nov. 2014.
[124] A. Salem and M. Narimani, "A review on multiphase drives for automotive traction applications," *IEEE Trans. Transport. Electrific.*, vol. 5, no. 4, pp. 1329–1348, Dec. 2019.
[125] A. Boglietti, R. Bojoi, A. Cavagnino, and A. Tenconi, "Efficiency analysis of PWM inverter fed three-phase and dual three-phase high frequency induction machines for Low/Medium power applications," *IEEE Trans. Ind. Electron.*, vol. 55, no. 5, pp. 2015–2023, May 2008.
[126] A. Negahdari, A. G. Yepes, J. Doval-Gandoy, and H. A. Toliyat, "Efficiency enhancement of multiphase electric drives at light-load operation considering both converter and stator copper losses," *IEEE Trans. Power Electron.*, vol. 34, no. 2, pp. 1518–1525, Feb. 2019.
[127] K. T. Chau, D. Zhang, J. Z. Jiang, C. Liu, and Y. Zhang, "Design of a magnetic-geared outer-rotor permanent-magnet brushless motor for electric vehicles," *IEEE Trans. Magn.*, vol. 43, no. 6, pp. 2504–2506, Jun. 2007.
[128] A. Toba and T. A. Lipo, "Novel dual-excitation permanent magnet Vernier machine," in *Proc. 34th IAS Annu. Meeting, Conf. Rec. IEEE Ind. Appl. Conf.*, Phoenix, AZ, USA, vol. 4, Oct. 1999, pp. 2539–2544.
[129] L. Sun, M. Cheng, and H. Jia, "Analysis of a novel magnetic-geared dual-rotor motor with complementary structure," *IEEE Trans. Ind. Electron.*, vol. 62, no. 11, pp. 6737–6747, Nov. 2015.
[130] M. Cheng, P. Han, and W. Hua, "General airgap field modulation theory for electrical machines," *IEEE Trans. Ind. Electron.*, vol. 64, no. 8, pp. 6063–6074, Aug. 2017.
[131] H. Huang and L. Chang, "Electrical two-speed propulsion by motor winding switching and its control strategies for electric vehicles," *IEEE Trans. Veh. Technol.*, vol. 48, no. 2, pp. 607–618, Mar. 1999.
[132] L. Tang, T. Burress, and J. Pries, "A reconfigurable-winding system for electric vehicle drive applications," in *Proc. IEEE Transp. Electrific. Conf. Expo (ITEC)*, Jun. 2017, pp. 656–661.

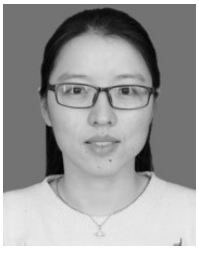

LINGYUN SHAO received the B.Sc. and Ph.D. degrees in electrical engineering from Southeast University, Nanjing, China, in 2012 and 2018, respectively. She is currently a Research Fellow of electric motor simulation and optimization with the University of Surrey, Guildford, U.K. Her research interests include the design and analysis of permanent magnet machines for electric propulsion systems and renewable energy generation.

AHU ECE HARTAVI KARCI received the M.Sc. and Ph.D. degrees in electrical engineering from Istanbul Technical University, Istanbul, Turkey, in 2000 and 2006, respectively. She is currently a Senior Lecturer with the University of Surrey, Guildford, U.K. Her research interests include intelligent control, electric vehicle modeling and control, and automated vehicles.

DAVIDE TAVERNINI received the M.Sc. degree in mechanical engineering and the Ph.D. degree in dynamics and design of mechanical systems from the University of Padova, Padua, Italy, in 2010 and 2014, respectively. During his Ph.D. degree, he was a part of the Motorcycle Dynamics Research Group. He is currently a Lecturer of advanced vehicle engineering with the University of Surrey, Guildford, U.K. His research interests include vehicle dynamics modeling and control, mostly applied to electric and hybrid electric vehicles.

ALDO SORNIOTTI (Member, IEEE) received the M.Sc. degree in mechanical engineering and the Ph.D. degree in applied mechanics from the Politecnico di Torino, Turin, Italy, in 2001 and 2005, respectively. He is currently a Professor of advanced vehicle engineering with the University of Surrey, Guildford, U.K., where he also coordinates the Centre for Automotive Engineering. His research interests include vehicle dynamics control and transmission systems for electric and hybrid electric vehicles.

MING CHENG (Fellow, IEEE) received the B.Sc. and M.Sc. degrees in electrical engineering from Southeast University, Nanjing, China, in 1982 and 1987, respectively, and the Ph.D. degree in electrical and electronic engineering from the University of Hong Kong, Hong Kong, in 2001. He is currently a Chair Professor with Southeast University, where he is also the Director of the Research Center for Wind Power Generation. Dr. Cheng is a fellow of the Institution of Engineering and Technology. He has served as the Chair and the Organizing Committee Member for many international conferences. He was a Distinguished Lecturer of the IEEE Industry Applications Society in 2015/2016.